

Impurity effect in multi-orbital, sign-reversing s-wave superconductors

Y. Nagai^{a,d,e}, K. Kuroki^{b,e}, M. Machida^{a,d,e}, H. Aoki^{c,e}

^aCCSE, Japan Atomic Energy Agency, 6-9-3 Higashi-Ueno, Taito-ku, Tokyo 110-0015, Japan

^bDepartment of Applied Physics and Chemistry, The University of Electro-Communications, Chofu, Tokyo 182-8585, Japan

^cDepartment of Physics, University of Tokyo, Hongo, Tokyo 113-0033, Japan

^dCREST (JST), 4-1-8 Honcho, Kawaguchi, Saitama 332-0012, Japan

^eTRIP (JST), 5 Sanbancho Chiyoda-ku, Tokyo 102-0075, Japan

Abstract

We study the impurity effects on the transition temperature T_c with use of the T -matrix approximation. We propose a way to visualize the multi-orbital effect by introducing the hybridization function characterizing the multi-orbital effect for the impurity scattering. Characterizing function does not depend on the superconducting pairing symmetry, since this function is defined by the eigenvectors in normal states. The result indicates that an impurity-robust superconductivity does not necessarily imply a sign-preserving pairing. Visualizing the hybridization effect in the effective five-band model for LaFeAsO, we show that the impurity effect on T_c is relatively weaker than that in single-band models.

Keywords: Impurity effects, Iron-based superconductors, multi-orbital systems 74.20.Rp, 74.70.Xa

1. Introduction

The discovery of the iron-based superconductor[1], which is a five-orbital system with three bands involved in the gap function[2], is stimulating renewed interests in multi-orbital superconductivity. Specifically, a sign-reversing s-wave pairing (s_{\pm}), which exploits the multi-orbital nature of the system, has been theoretically proposed as a candidate[2, 3]. While various experimental measurements for determining the pairing symmetry in the iron-based superconductors are accumulating, which include the penetration depth, thermal conductivity, ARPES, STM, and NMR, one important test is the impurity effect on superconducting transition temperature T_c . This has in fact been studied intensively both experimentally and theoretically [4–7]. There are two trends found in the experiments on the non-magnetic impurity effect on T_c for LaFe_{1-x}Zn_xAsO. The experiment by Li *et al.* suggests that the doping of Zn in LaFeAsO_{1-y}F_y does not reduce T_c [4]. The result by Guo *et al.* suggests that T_c decreases significantly for a minimal level of Zn doping in LaFeAsO_{0.85}[5]. A theoretical work by Onari and Kontani suggests that a fully gapped sign-reversing s-wave state is very fragile against non-magnetic impurities[7]. On the other hand, the compound containing phosphorus, LaFePO, whose gap function has line-nodes, is robust against non-magnetic impurities[8]. With this background, here we theoretically study the problem from a broader context, i.e., we want to identify which factors are crucial in determining T_c in dirty, multi-orbital superconductors, especially for the sign-reversing s-wave.

2. Formulation

The self-energy in the T -matrix approximation in the orbital-representation is expressed as $\check{\Sigma}^{\text{orbital}} = n_{\text{imp}}\check{T}$, where n_{imp} is

the density of impurities, and $\check{T} = (\check{I} - \check{V}\check{G}_{\text{loc}})^{-1}\check{V}$. Here $\check{V} = \check{V}\check{\sigma}_z$, and the local Green's function \check{G}_{loc} is defined as $\check{G}_{\text{loc}} = \frac{1}{N} \sum_{\mathbf{q}} \check{G}^{\text{orbital}}(\mathbf{q})$ with

$$\check{G}^{\text{orbital}}(\mathbf{q}, i\omega_n) \equiv \begin{pmatrix} \hat{G}^{\text{orbital}}(\mathbf{q}, i\omega_n) & -\hat{F}^{\text{orbital}}(\mathbf{q}, i\omega_n) \\ -\hat{F}^{\text{orbital}\dagger}(\mathbf{q}, i\omega_n) & -\hat{G}^{\text{orbital}}(\mathbf{q}, -i\omega_n) \end{pmatrix}. \quad (1)$$

Throughout the paper, \hat{a} denotes an $n \times n$ matrix in the orbital space while \check{a} a $2n \times 2n$ matrix composed of the 2×2 Nambu space and the $n \times n$ orbital space. With use of the unitary matrix $\check{P}_{\mathbf{k}}$ that diagonalizes the Hamiltonian in the orbital basis, the self-energy in the band representation is expressed as $\check{\Sigma}_{\mathbf{k}}^{\text{band}} = n_{\text{imp}}[\check{I} - \check{V}^{\text{band}}(\mathbf{k})\check{G}_{\text{loc}}^{\text{band}}(\mathbf{k})]^{-1}\check{V}^{\text{band}}(\mathbf{k})$ with $\check{V}^{\text{band}}(\mathbf{k}) \equiv \check{P}_{\mathbf{k}}^{\dagger}\check{V}\check{P}_{\mathbf{k}}$. Considering the orbital-independent impurity potential $\check{V} = V_0\check{\sigma}_z$ introduced in Ref. [7], the self-energy is expressed as $\check{\Sigma}_{\mathbf{k}}^{\text{band}} = n_{\text{imp}}[\check{I} - V_0\check{\sigma}_z\check{G}_{\text{loc}}^{\text{band}}(\mathbf{k})]^{-1}V_0\check{\sigma}_z$. We then obtain the diagonal elements of the normal part of the self-energy as

$$(\hat{\Sigma}_{\mathbf{k}}^{\text{band}, N})_{ii} = V_0 + V_0^2(\hat{G}_{\text{loc}}^{\text{band}})_{ii}(\mathbf{k}) + \dots, \quad (2)$$

with

$$(\hat{G}_{\text{loc}}^{\text{band}})_{ii}(\mathbf{k}) = \frac{1}{N} \sum_{\mathbf{q}} \sum_l |C_{li}(\mathbf{q}, \mathbf{k})|^2 G_l^{\text{band}}(\mathbf{q}). \quad (3)$$

Here we have introduced a unitary matrix $\hat{C}(\mathbf{q}, \mathbf{k})$ whose element $C_{ij}(\mathbf{q}, \mathbf{k})$ can be written as

$$C_{ij}(\mathbf{q}, \mathbf{k}) = \vec{p}_{qi}^{\dagger} \vec{p}_{kj}, \quad (4)$$

where \vec{p}_{kj} denotes the j -th eigenvector of the Hamiltonian with momentum \mathbf{k} in the normal state, while \mathbf{k} and \mathbf{q} denote, respectively, the initial- and final-state quasiparticle momenta in

impurity scatterings. Equations (2) and (3) imply that the l -th band hybridization affects the i -th band self-energy ($\hat{\Sigma}_k^{\text{band},N}$)_{ii} through $|C_{li}(\mathbf{q}, \mathbf{k})|^2 G_{li}^{\text{band}}(\mathbf{q})$. Hence the factor $|C_{li}(\mathbf{q}, \mathbf{k})|^2$ characterizes the multi-orbital effect for the impurity scattering. From Eq. (4) we find that the more the eigenvectors with initial-state momentum \mathbf{k} and final-state momentum \mathbf{q} resemble with each other, the stronger the inter-band impurity effect on T_c becomes.

Thus a speciality of a multi-band system is that, on top of the band dispersion and Fermi surface, the character of eigenvectors acts as an important factor determining the way in which the impurity effect appears. We can thus call the factor $|C_{li}(\mathbf{q}, \mathbf{k})|^2$ the *impurity scattering intensity*. We can use this property to construct a model that is robust against the impurity effect. For instance, the impurity effect does not appear on T_c in a two-orbital model described by $H_k^{ii} = -[\cos(k_x) + \cos(k_y)]$, $H_k^{ij} = t'$, since the impurity scattering intensity in this case reduces to $|C_{li}(\mathbf{q}, \mathbf{k})|^2 = \delta_{li}$ everywhere in momentum space.

3. Visualized hybridization effect on the impurity scattering

The general scheme above enables us to visualize the hybridization effect on the impurity scattering. In doing so, we can concentrate on the Fermi momentum, since the Green function has amplitudes localized around the Fermi energy in Eq. (3). Then $|C_{li}(\mathbf{q}, \mathbf{k})|^2$ can be parameterized as $|C_{li}(\theta_l, \theta_i)|^2$, where θ_{li} describes the position of the final- (initial-) state on the l -th (i -th) Fermi surface. Let us visualize the hybridization effect in the effective five-band model proposed by Kuroki *et al.* for LaFeAsO [2]. In this model with the Fermi energy $E_F = 10.94\text{eV}$, there are two hole Fermi pockets around $(k_x, k_y) = (0, 0)$, and two electron pockets around $(0, \pi)$ and $(\pi, 0)$ as displayed in Fig. 1.

First, we visualize the *inter-band* impurity scattering intensity of the quasiparticles between the hole and electron Fermi surfaces. Here, we introduce the band-index i whose energy ϵ_i satisfies the relation $\epsilon_i > \epsilon_j$ ($i > j$). The hole Fermi surfaces on the 2nd and 3rd bands are mainly constructed from d_{xz} and d_{yz} orbitals. The dominant component of the eigenvectors at the electron Fermi surface on the 4th band depends on the Fermi wave-number. In Fig. 3, we show the dominant components in the orbital basis on each Fermi surface. In the case of the impurity scattering between 2nd and 4th bands, the intensity strongly depends on both of the initial-state θ_2 and the final-state θ_4 as shown in Fig. 2(a). For example, the intensity at $(\theta_2, \theta_4) = (3\pi/2, \pi/2)$ is almost zero, so that the inter-band impurity scatterings between $\theta_2 = 3\pi/2$ and $\theta_4 = \pi/2$ do not affect the superconducting transition temperature T_c even if these are sign-reversing scatterings. The intensity at $(\theta_2, \theta_4) = (\pi/2, \pi)$ as shown in Figs. 2 (a) and 3 has a maximum value $|C_{24}(\theta_2, \theta_4)|^2 \simeq 0.6$. By contrast, the impurity scattering between 3rd and 4th bands does not affect T_c regardless of the initial and final momenta, since the intensity is small everywhere as shown in Fig. 2(b).

Second, we turn to the *intra-band* impurity scattering intensity $|C_{22}(\theta_2, \theta_2')|^2$ and $|C_{33}(\theta_3, \theta_3')|^2$. As shown in Fig. 4,

the intensities on a same band are bigger than that between different bands on the whole. On the line satisfying the relation $\theta_i = \theta_i'$, the intensity $|C_{ii}(\theta_i, \theta_i)|^2$ become $|C_{ii}(\theta_i, \theta_i)|^2 = 1$, since the eigenvectors are same. The intensities $|C_{ii}(\theta_i, \theta_i + \pi)|^2$ differ from $|C_{ii}(\theta_i, \theta_i)|^2 = 1$. This originates from an absence of the inversion symmetry in the eigenvector \vec{p}_{kj} . Although this may first seem strange, the Hamiltonian for momentum \mathbf{k} in the orbital-basis is not equal to that for momentum $-\mathbf{k}$, since the positional relation between the iron atoms and the arsenic atoms differs between the directions for \mathbf{k} and $-\mathbf{k}$.

From these figures 2 and 4 we find that the impurity scattering intensities $|C_{li}(\theta_l, \theta_i)|^2$ in this effective five-band model are small on the whole. Focusing the fact that the intensities in single band models are always $|C_{11}(\theta_1, \theta_1)|^2 = 1$, these figures suggest that the impurity effect on T_c in the effective five-band model is relatively weaker than that in single-band models.

Finally, we show the impurity intensity dependence of T_c in Fig. 5 with use of the self-consistent T -matrix approximation in the sign-reversing s -wave superconductor for an impurity density $n_{\text{imp}} = 0.01$. The result, which is essentially the same as the result in Ref. [7], indicates that an attractive impurity potential does not significantly reduce T_c . This behavior originates, in the present view, from the multi-orbital hybridization effect characterized by $|C_{li}(\theta_l, \theta_i)|^2$.

4. Conclusion

We have studied the impurity effects on T_c with use of the T -matrix approximation. We found that the hybridization function $|C_{li}(\mathbf{q}, \mathbf{k})|^2$ (Eq. (4)) characterizes the multi-orbital effect for the impurity scatterings. The more the eigenvectors at initial-state and final-state momenta are similar to each other, the stronger the inter-band impurity effect on T_c becomes. We thus proposed a way to visualize the multi-orbital effect. The figures visualizing the multi-orbital effect suggest that the impurity effect on T_c in the effective five-band model is relatively weaker than that in single-band models. The above results do not depend on the superconducting pairing symmetry, since $|C_{li}(\mathbf{q}, \mathbf{k})|^2$ is defined only by the eigenvectors in normal states. The message of this result is that there can be impurity-robust sign-reversing s -wave pairing symmetry in the iron-based superconductors. Conversely, an impurity-robust superconductivity does not necessarily imply sign-preserving pairing. In addition, with use of the present visualization, one might find the pairing symmetry with line-nodes where the impurity effects do not appear on T_c in such materials as LaFePO.

References

- [1] Y. Kamihara, T. Watanabe, M. Hirano, and H. Hosono, J. Am. Chem. Soc. 130 (2008) 3296.
- [2] K. Kuroki, S. Onari, R. Arita, H. Usui, Y. Tanaka, H. Kontani, and H. Aoki, Phys. Rev. Lett. 101 (2008) 087004.
- [3] I. I. Mazin, D. J. Singh, M. D. Johannes, and M. H. Du, Phys. Rev. Lett. 101 (2008) 057003.
- [4] Y. K. Li, X. Lin, Q. Tao, C. Wang, T. Zhou, L. J. Li, Q. B. Wang, M. He, G. H. Cao, and Z. A. Xu, New J. Phys. 11, (2009) 053008.

- [5] Y. F. Guo, Y. G. Shi, S. Yu, A. A. Belik, Y. Matsushita, M. Tanaka, Y. Katsuya, K. Kobayashi, I. Nowik, I. Felner, V. P. S. Awana, K. Yamaura, and E. Takayama-Muromachi, Phys. Rev. B 82 (2010) 054506.
- [6] M. Sato, Y. Kobayashi, S. C. Lee, H. Takahashi, E. Satomi, and Y. Miura, J. Phys. Soc. Jpn. **79** (2010) 014710.
- [7] S. Onari and H. Kontani, Phys. Rev. Lett. 103 (2009) 177001.
- [8] S. Suzuki, S. Miyasaka and S. Tajima, JPS Annual meetings (2010), 23pGH-2.

Figure captions

Figure 1: Fermi surfaces in the effective five-band model at the Fermi energy $E_F = 10.94$ eV.

Figure 2: Inter-band impurity scattering intensity of the quasi-particles between the 2nd band and the 3rd band (a), or between 2nd band and 4th band (b).

Figure 3: Dominant character of the eigenvectors is schematically shown on the Fermi surfaces. The different colors denote different hybridization in the orbital basis. Blue dots represent an example of the initial and final momenta.

Figure 4: Intra-band impurity scattering intensity on the 2nd band (a), or on the 3rd band (b).

Figure 5: Impurity-intensity (I) dependence of T_c in the sign-reversing s -wave superconductor.

Figures

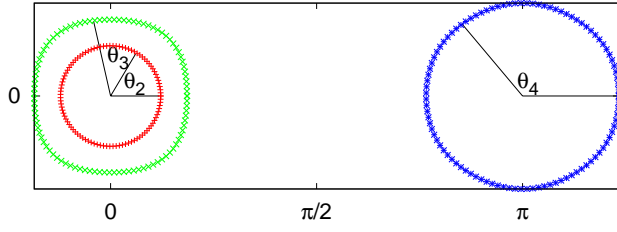


Figure 1:

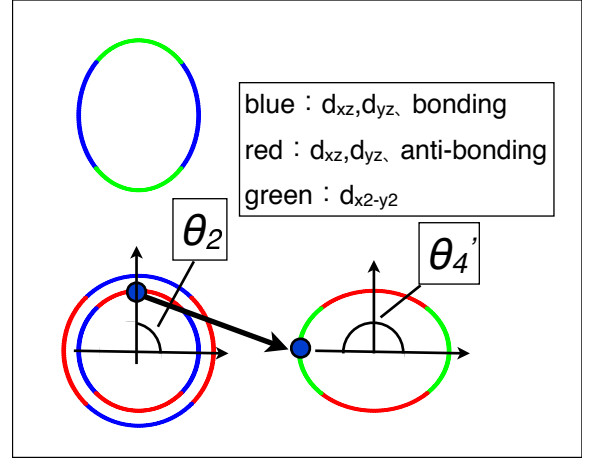


Figure 3:

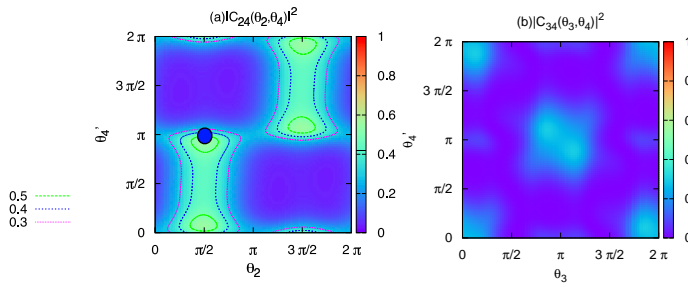


Figure 2:

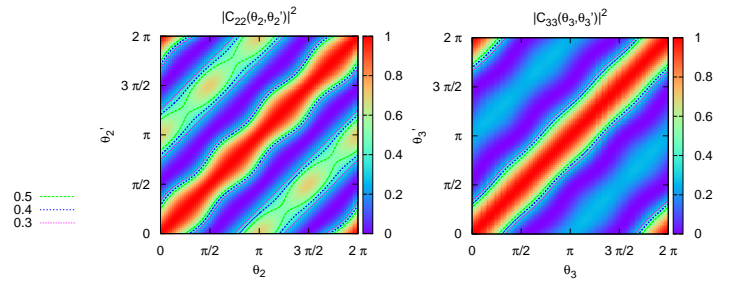


Figure 4:

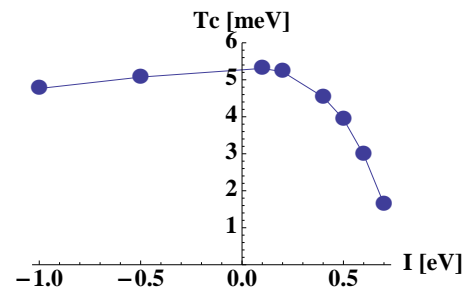


Figure 5: